Synthesis of Calcium Carbonate–Chitosan Composites via Biomimetic Processing

SUKUN ZHANG[1] and K. E. GONSALVES[1,2,*]

[1]Polymer Science Program of the Institute of Materials Science and [2]Department of Chemistry, U-136, University of Connecticut, Storrs, Connecticut 06269

SYNOPSIS

The crystal growth of calcium carbonate on a chitosan substrate was achieved using a supersaturated calcium carbonate solution, at different concentrations of polyacrylic acid (PAA) as an additive. Several techniques have been employed to characterize the systems. The pH of the solution as the one of indices was used to monitor the crystallization. In the absence of polyacrylic acid, the pH of the solution changed from 6.00 to 8.50 during the crystallization; meanwhile, sporadic nucleation and crystallization was observed via optical microscopy. By introducing polyacrylic acid to the systems, positively charged protonated nitrogen and negatively charged carboxylate ions were produced by reaction between the amino group in chitosan and the carboxyl group in polyacrylic acid, which were detected by ATR-IR and XPS techniques. These charges induced calcium carbonate nucleation of calcite and vaterite crystals on the chitosan–film surface. The average size of the vaterite phase was about 15 nm, determined by XRD. The pH of the solution changed from 5.80 to 9.25 during the crystallization; moreover, the crystals showed spherical morphology, which consisted of a large number of small particles with a diameter of about 0.2 μm.

INTRODUCTION

Ceramic–polymer composites produced by natural organisms are known to have properties far beyond those that can be achieved in present technological materials.[1] The mollusk shell, for example, starting with relatively weak structural ingredients, calcium carbonate and chitin, is one such ceramic–polymer composite. In nacre, the overall composite is more than 95 volume percent calcium carbonate, with the remainder an organic matrix of protein and chitin. The inorganic phase consists of highly oriented aragonite platelets forming the bricks and the organic matrix forming the mortar in between.[1] Even though nacre consists of a high amount of the inorganic component, it has excellent fracture toughness and high strength. Bone, another ceramic–polymer composite, contains collagen and an inorganic mineral phase, hydroxyapatite. The bone mineralization is a complicated process controlled by many factors. Initially calcium phosphate is deposited in the holes of the collagen fibrils and later fills in the pores and the rest of the space within the collagen fibrils. The crystals have the form of thin plates about 50 × 25 × 3 nm.[2,3]

Instead of trying to duplicate the entire biomineralization process, scientists are dividing the process into stages that can be understood and adapted to practical processing schemes.[3] Hydroxyapatite crystallization from an aqueous solution on decalcified collagen has been reported by Weiner and coworkers.[4] Sikes and Wheeler have tested the effect of a variety of acid-containing peptides on calcium carbonate crystallization by using the kinetic approach.[5] Compressed Langmuir monolayers have also been used for controlling the crystallization of calcium carbonate.[6] Kinetic studies of hydroxyapatite crystallization on various substrates have been

* To whom correspondence should be addressed.

Journal of Applied Polymer Science, Vol. 56, 687–695 (1995)
 CCC 0021-8995/95/060687-09

reported by Koutsoukos and Nancollas et al.[7] Stupp and his co-workers have synthesized organoapatites by nucleation and growth of apatite crystals in media containing poly(amino acids) or synthetic organic polyelectrolytes.[8] Most of these studies have been conducted to understand the factors that control the nucleation and orientation of crystallization. However, very limited knowledge about the ceramic–polymer interfaces, structure, chemistry, and whether the interfacial interaction involves ion binding is known.

To model nacre we have chosen chitosan, in which free amino groups exist, as a substrate and low molecular weight polyacrylic acid as an additive instead of complex proteins. The crystal growth of calcium carbonate on a chitosan substrate has been achieved using a supersaturated solution of calcium carbonate at different concentrations of polyacrylic acid. Several techniques have been employed to characterize the systems, such as x-ray diffraction (XRD), x-ray photoelectron spectroscopy (XPS), and attenuated total reflectance infrared spectroscopy (ATR). By producing charges, ion binding involved in the nucleation and crystallization, the interfacial interactions between ceramic and polymer have been investigated.

EXPERIMENTAL

Preparation of Calcium Carbonate Supersaturated Solution

The supersaturated calcium bicarbonate solution was prepared following the procedure described by Mann.[6] A suspension of $CaCO_3$ (calcite), with the ratio 0.9/100 (mg/mL) of calcium carbonate to distilled water, was first prepared. While stirring, CO_2 was bubbled into the system at room temperature and kept for 6 h. The suspension was then filtered and the filtrate purged with CO_2 gas for 30 min to dissolve any remaining crystals. The pH of the resulting supersaturated solution was about 6.00.

Preparation of Chitosan Films

A chitosan film was obtained by casting the 1% (w/w) solution of chitosan (Sigma Co.) in 1% (w/w) acetic acid aqueous solution on a polymethylmethacrylate plate or a glass slide. In a typical preparation of the casting solution, 2 g of chitosan was added in 100 mL of distilled water and stirred for 10 min. Then 100 g of 2% (w/w) acetic acid was added and stirred at room temperature for another 30 min.[9] A

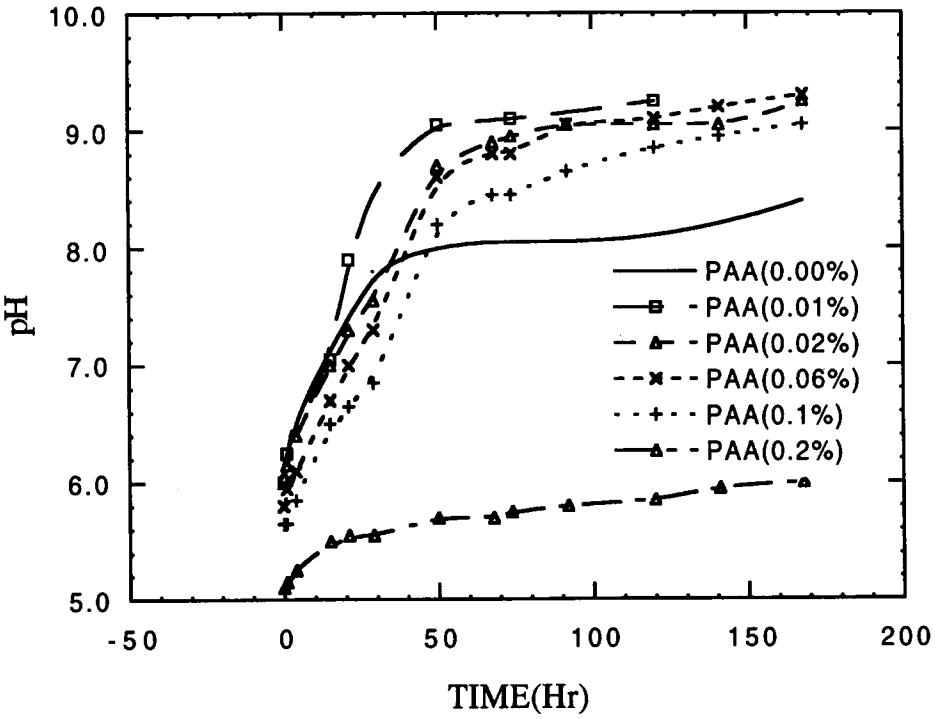

Figure 1 pH of supersaturated calcium carbonate solutions as functions of crystallization time at the different concentrations (wt %) of polyacrylic acid (20°C).

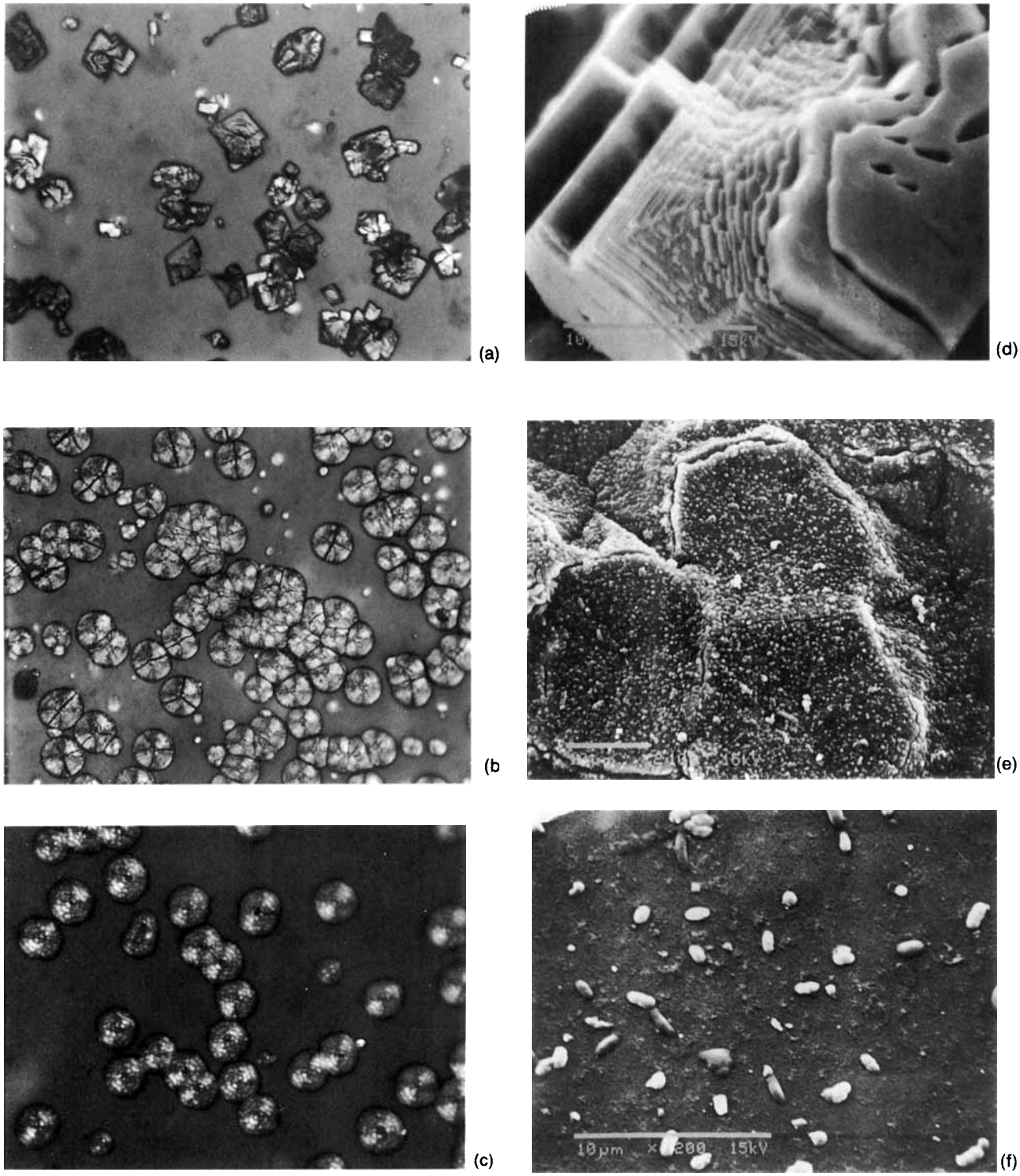

Figure 2 OM and SEM pictures of calcium carbonate crystals on chitosan–film surfaces: (a) 0.00% PAA, pH = 8.50 (OM); (b) 0.02% PAA, pH = 9.10 (OM); (c) 0.06% PAA, pH = 9.10 (OM); (d) 0.00% PAA, pH = 8.5 (SEM); (e) 0.02% PAA, pH = 9.25 (SEM); (f) 0.1% PAA, pH = 9.00 (SEM).

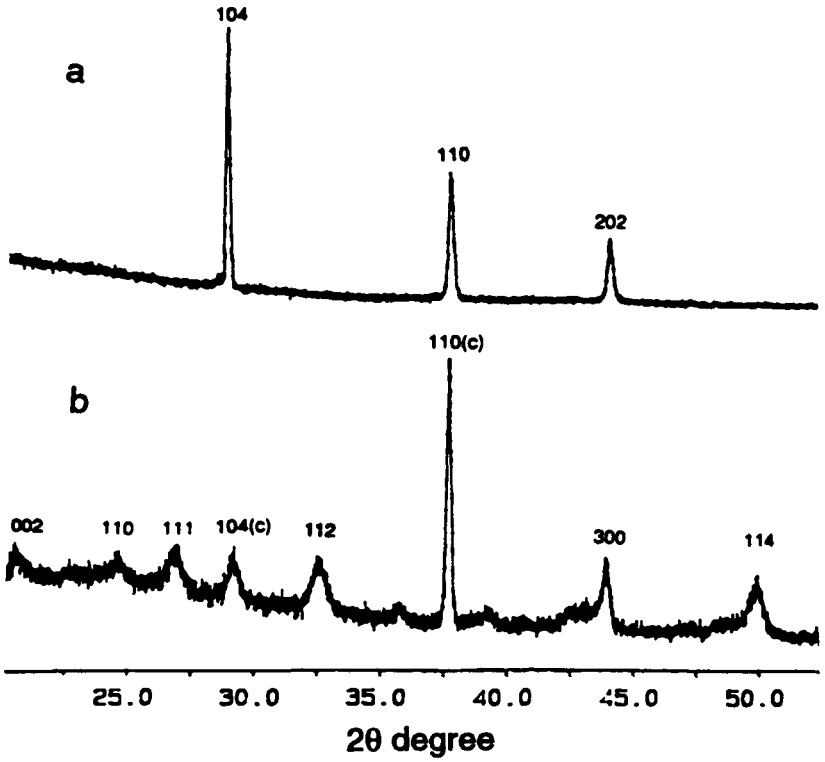

Figure 3 X-Ray patterns of calcium carbonate: (a) with 0.00% PAA in the system; (b) with 0.02% PAA in the system.

viscous solution was obtained and filtered. The chitosan film made in this way was then neutralized with dilute ammonium hydroxide and washed extensively with water. After air drying, it was further dried under vacuum at room temperature.

Polyacrylic acid (Aldrich Co.) with molecular weight 2,000 was employed as an additive. Various amounts of the polyacrylic acid were weighed and placed into polystyrene (PS) bottles before adding the calcium carbonate supersaturated solution.

Characterization

The pH of solution was measured by a Fisher pH meter (model 107). $CaCO_3$ crystallite sizes and morphology were observed under a polarized optical microscope, model Nikon Labophot-pol, and a scanning electron microscope (SEM, AMR 1200B). X-Ray diffraction (XRD) was carried out to determine the crystallite sizes and phases. The surfaces of chitosan films, with or without soaking in polyacrylic acid solution, were examined by attenuated total reflectance infrared spectroscopy (ATR-IR, Mattson Polaris) by using a 60° Germanium analyzer. X-Ray photoelectron spectroscopy (XPS) was used to detect the surface structures of chitosan films. XPS spectra were collected on a monochromatic spectrometer (Perkin-Elmer, 5300) using Al Kα source (600 W, 15 KeV) with the pass energy 37.5 eV. The vacuum was maintained at approximately 1×10^{-9} torr.

RESULTS AND DISCUSSION

Crystallization of $CaCO_3$ was controlled by the following equilibrium in which carbon dioxide is continually lost:

$$Ca^{2+}\ (aq) + 2HCO_3^-\ (aq) \rightleftharpoons CaCO_3\ (s) + CO_2\ (g) + H_2O\ (l) \quad (1)$$

On the evolution of carbon dioxide gas from the solution, the pH of the supersaturated solution increased. Figure 1 shows the result of six systems with different concentrations (all in weight fraction) of polyacrylic acid. As the crystallization proceeded, the pH of solution increased and finally leveled off to a plateau. Three such plateaus were obtained.

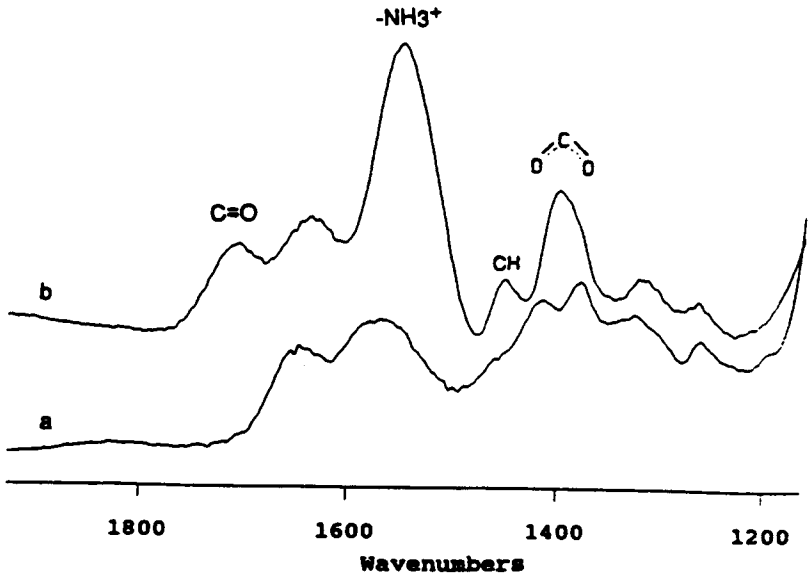

Figure 4 ATR spectra of chitosan–film surface: (a) without polyacrylic acid; (b) soaked in 0.2% PAA aqueous solution for 3 h.

First, in the absence of polyacrylic acid, the pH value increased as the crystallization of $CaCO_3$ proceeded. After 40 h it was up to a plateau of about 8.0. Crystallization was complete at a pH of about 8.50, and the XRD pattern showed that calcite was formed [Fig. 3(a)]. The calcium carbonate crystals appeared as a multilayer habit, precipitating on the chitosan film randomly and sporadically [Fig. 2(a), (d)]. The crystals also occurred on the air/water interface as well as the inner edge of the container in the same formation. In the presence of polyacrylic acid, the pH values of the solutions increased as crystallization proceeded and leveled off to different plateau values, depending on the polyacrylic acid concentration. At low concentrations, such as 0.01% (wt) and 0.02% (wt), the pH increased as fast as in the case without polyacrylic acid in the first 30 h. After that, the pH values increased rapidly and leveled off to a plateau of about 9.10. At a concentration of 0.06%, crystallite nucleation and growth were inhibited at the beginning, resulting in a lower pH than that of the lower polyacrylic acid concentrations. Eventually, the pH of the solution went up to 9.25. Because the dissociation constant of polyacrylic acid is 4.5,[10] the acid groups of polyacrylic acid are mostly in the form of —COO— carboxylate ions at a pH range of 5.8 to 9.25. Thus, for the polyacrylic acid concentration of 0.1%, although its pH eventually got to 9.00, crystallization was mostly inhibited by mobile polyacrylic acid carboxylate ions in the solution, and only a few crystals grew on the chitosan film [Fig. 2(f)]. When the concentration of polyacrylic acid was 0.2%, crystallization was totally inhibited, and the pH of the solution remained at 6.00 and no crystals were observed on the chitosan film surface. At lower concentrations of PAA, the crystal shapes and habits were different from those obtained without polyacrylic acid. Crystals only appeared on the chitosan film and showed spherical symmetry around a center of nucleation [Fig. 2(b, c)].

In the absence of the polyacrylic acid, only calcite appears in the XRD pattern. On the other hand, in the presence of the polyacrylic acid, the XRD pattern shows that a mixture of calcite and vaterite was formed. The high and sharp peak at $2\theta = 37.6°$ and small peak at $2\theta = 28.8°$ represent (110) and (104) planes of calcite, respectively; the remaining peaks pertain to planes of vaterite.

The crystallite sizes of vaterite phase were calculated from the half-peak width of the XRD according to the following equation[11]:

$$t = 0.9\lambda/B \cos\theta, \quad B^2 = B_r^2 + B_i^2 \qquad (2)$$

where t is average crystallite size, λ is the wavelength of copper (1.54 Å), B is the width of the half-height peak, and θ is the diffraction angle. B is the width measured from x-ray pattern, B_r is the actual width of a sample, and B_i is the width caused by the instrument. Because the peak of calcite 110 plane is very sharp, it was considered to be the width caused by the

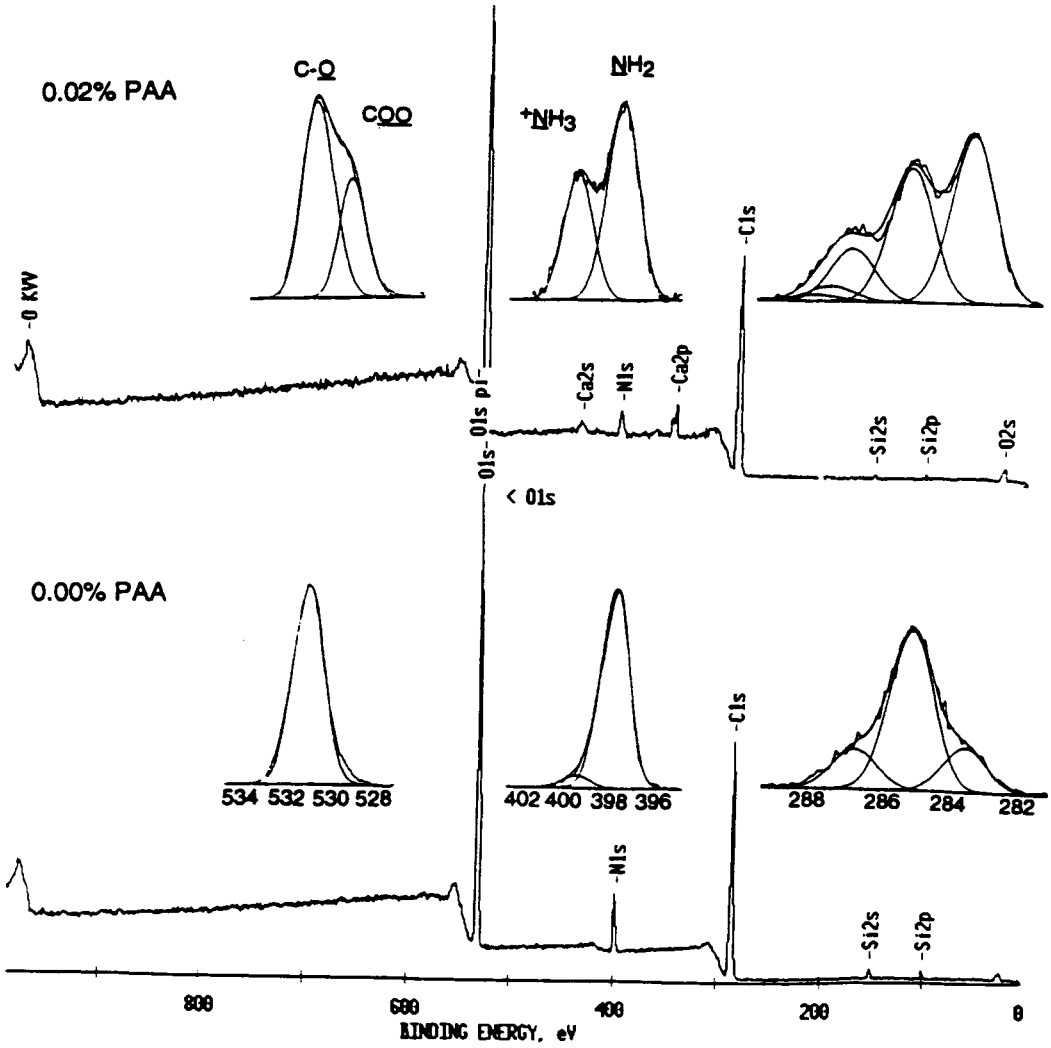

Figure 5 XPS wide scan and core-level spectra of chitosan–film surfaces soaked in the supersaturated calcium carbonate aqueous solutions at different concentrations of polyacrylic acid for 4 h.

instrument. By picking several vaterite peaks, the average crystallite size of vaterite was calculated using Eq. (2). As a result, the average crystallite size t of vaterite was about of 15 nm. Also, in the presence of polyacrylic acid, as the crystallization proceeded, the crystallites covered the whole chitosan film [Fig. 3(d)].

Table I Atomic Concentrations of Carbon, Oxygen, Nitrogen, and Calcium of Chitosan–Film Surface at Different Concentration of Polyacrylic Acid

Conc. of PAA (%)	C (AC %)	O (AC %)	N (AC %)	Ca (AC %)	N/N^+ (AC/AC)	PAA/Chitosan (Repeat Unit Ratio)
0.00	55.43	36.27	8.30	0.00	95/5	0.0
0.01	56.32	38.02	4.64	1.00	50/50	2.62
0.02	57.75	37.15	4.12	0.97	62/38	2.50
0.06	56.89	38.26	3.66	1.18	51/49	3.23
0.1	59.06	37.40	3.54	—	50/50	3.28

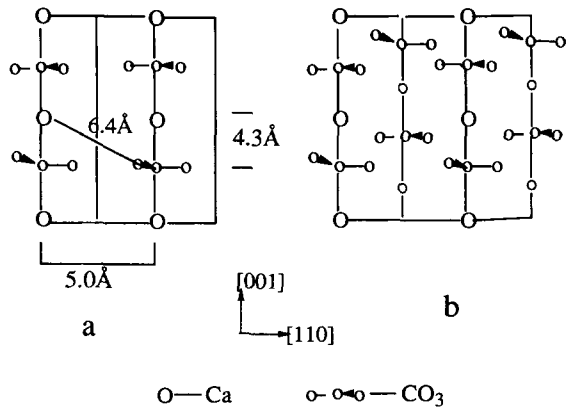

Figure 6 Cell projections for calcite: (a) parallel to the (110) axis only coplanar atoms in the (110) face; (b) parallel to the (110) axis with additional noncoplanar atoms.[4]

The ATR spectra of chitosan–film surfaces are shown in Figure 4. Sample A is the one without soaking in the polyacrylic acid aqueous solution, and sample B is soaked in a 0.2% polyacrylic acid aqueous solution for 3 h. A new band at 1707 cm^{-1} appearing in sample B corresponds to the carbonyl C=O stretching absorption of the carboxyl group in polyacrylic acid. The band appearing at 1550 cm^{-1} in the spectrum can be assigned to a symmetric $-NH_3^+$ deformation, and broad bands appearing at 2500 cm^{-1} and 1900 cm^{-1} confirm the presence of $-NH_3^+$ on the chitosan film.[12] Another new band at 1400 cm^{-1} represents the carboxylate ion. Thus, the negatively charged carboxylate ion and positively charged $-NH_3^+$ coexist on the chitosan–film surface in the presence of polyacrylic acid. This was also confirmed by XPS analysis.

Figure 5 shows a series of XPS 0–1000 eV wide scan and core-level spectra of the chitosan–film surfaces after being soaked in supersaturated calcium carbonate aqueous solution for 4 h under a series of concentrations of polyacrylic acid. In the absence of polyacrylic acid, only one kind of nitrogen and oxygen appears. Three types of carbon detected in this case represent O—C—O, C—C—O, and C–N, respectively.[13–15] Their area ratio is 1 : 4 : 1, which matches the ratio of the chitosan repeat unit. The absence of calcium element in this situation indicates that no calcium carbonate nuclei formed at the beginning of the crystallization. In the presence of polyacrylic acid, on the other hand, two peaks occurred at binding energies about 400 eV and 398 eV, which represent protonated nitrogen and free-base nitrogen, respectively. The other two peaks detected at binding energies about 531 eV and 530 eV pertain to the oxygen of —C—O—C of chitosan and —C=O of polyacrylic acid, respectively. The appearance of calcium element in the XPS spectra results from the nucleation of calcium carbonate on the chitosan–film surface in the presence of polyacrylic acid. In this case, the positive and the negative charges occur on the chitosan film.

Table I summarizes both the atomic concentrations of elements and the repeat-unit ratios of chitosan to polyacrylic acid on the chitosan–film surface at the different concentrations of polyacrylic acid. The atomic concentration ratios of free nitrogen to protonated nitrogen were around 1 : 1 after adding polyacrylic acid into the systems. The atomic concentration of nitrogen decreased dramatically after adding polyacrylic acid into the system and decreased slightly as the concentration of polyacrylic acid increased, while the repeat-unit ratio of polyacrylic acid to chitosan showed the opposite trend. Therefore, the higher the concentration of polyacrylic acid, the more the polyacrylic acid was adsorbed onto the chitosan–film surface. However, above 0.06 wt %, the adsorption appeared to come to equilibrium. At the concentration of 0.1 wt %, there were more mobile carboxylate anions of polyacrylic acid in the solution, which inhibited the crystallization.

The crystallographic orientation can be estimated by an atomic matching at the interface of the organic matrix and inorganic minerals. In the presence of polyacrylic acid, the XRD pattern gave a high and sharp peak at $2\theta = 37.6°$, corresponding to 110 plane of calcite. This indicated that calcite crystals were preferentially oriented with the 110 plane parallel to the chitosan film. The Ca-Ca distance of calcite

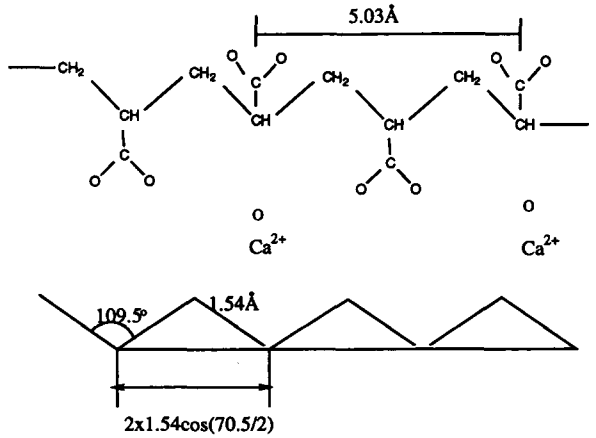

Figure 7 Scheme for the conformation of polyacrylic acid on the chitosan–film surface.

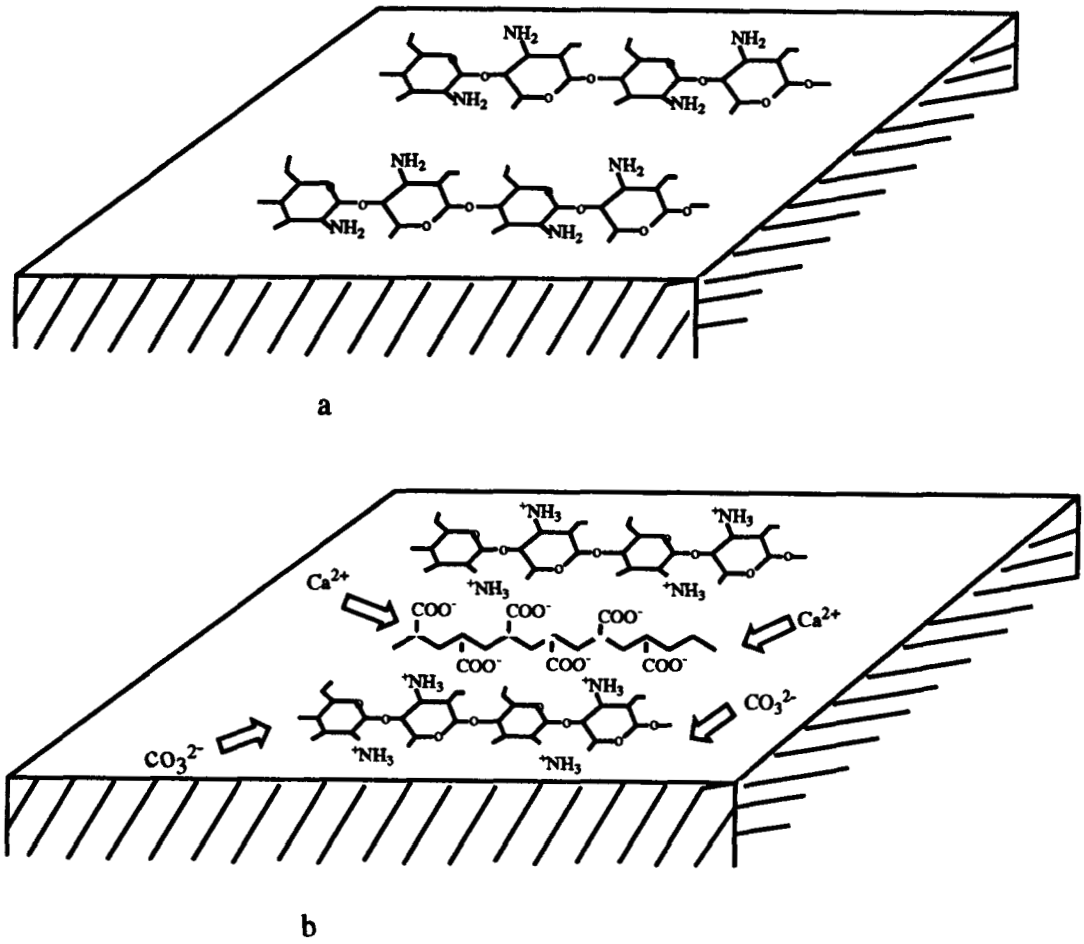

Figure 8 Scheme for the structure of chitosan–film surface: (a) in the absence of polyacrylic acid; (b) in the presence of polyacrylic acid.

is about 5.0 Å on the (110) plane (Fig. 6).[6] In the zig-zag conformation, the distance of two carboxylate ions in polyacrylic acid is 5.03 Å (Figs. 7 and 8), which matches the lattice of the (110) plane of calcite. Thus, Ca binding to negatively charged carboxylate ions in polyacrylic acid results in the nucleation of the (110) plane of calcite.

CONCLUSIONS

Introducing polyacrylic acid to the system for biomimetic growth of calcium carbonate crystals on a chitosan–film surface results in creating protonated nitrogens and carboxylate anions on the chitosan–film surface. Nucleation is initiated from these charges. At low concentrations of polyacrylic acid, nucleation and crystallization occurred and crystals covered the whole film with a spherical morphology. At higher concentration, such as 0.1%, even though nucleation did occur, crystallization was inhibited by the mobile carboxylate anions of polyacrylic acid in the solution.

REFERENCES

1. M. Sarikaya and I. A. Aksay, *Structure, Cellular Synthesis and Assembly of Biopolymers,* S. Case, Ed., Springer Verlag, Amsterdam, 1992, pp. 1–25.
2. M. J. Glimchere, *The Chemistry and Biology of Mineralized Connective Tissues,* Elsevier/North-Holland, Amsterdam, 1981, p. 617.
3. B. C. Bunker, P. C. Rieke, et al., *Science,* **264,** 48–55 (1994).
4. S. Weiner and L. Addadi, *Trends Biochem. Sci.,* **16**(7), 252–256 (1988).
5. A. P. Wheeler, K. W. Rusenko, D. M. Swift, and C. S. Sikes, *Marine Biol.,* **98,** 71 (1988).

6. S. Mann, *Nature,* **334,** 692–695 (1988); *Struct. Bonding,* **54,** 125–174 (1983); *J. Chem. Soc. Faraday,* **86,** 1873–1880 (1990).
7. P. G. Koutsoukos and G. H. Nancollas, et al., *J. Cryst. Growth,* **57,** 325 (1982); *J. Am. Chem. Soc.,* **102**(5), 1553 (1980); *J. Phys. Chem.,* **85,** 2403 (1981); *J. Colloid Interface Sci.,* **127,** 273 (1989).
8. S. I. Stupp, et al., *J. Mater. Res.,* **7,** 2599 (1992); *J. Biomed. Mater. Res.,* **26,** 169–183 (1992); *J. Biomed. Mater. Res.,* **27,** 289–299 (1993); *J. Biomed. Mater. Res.,* **27,** 301–311 (1993).
9. P. R. Austin and D. Wilmington, US Pat. 4,309,534 (1982).
10. S. Chibowski, *J. Colloid Interface Sci.,* **140**(2), 444–449 (1990).
11. B. D. Cullity, *Elements of X-Ray Diffraction,* Addison-Wesley, Reading, MA, 1956.
12. F. G. Pearson, *J. Polym. Sci.,* **XLIII,** 101–116 (1960).
13. C. D. Wagner, *Handbook of X-Ray Photoelectron Spectroscopy,* Perkin-Elmer, Eden Prairie, MN, 1979.
14. J. D. Andrade, *Surface Interfac. Aspects Biomed. Polym.,* **1,** Chapt. 5 (1985).
15. D. T. Clark, *Polymer Surfaces,* D. T. Clark and W. J. Feast, Eds., Wiley & Sons, New York, 1978.

Received June 27, 1994
Accepted October 7, 1994